07/17

Eur. Phys. J. Appl. Phys. **37**, 229–235 (2007)
DOI: 10.1051/epjap:2007010

THE EUROPEAN PHYSICAL JOURNAL APPLIED PHYSICS

On Reynolds number and scaling effects in microchannel flows

J. Yao[1], Y.F. Yao[1,a], M.K. Patel[2], and P.J. Mason[1]

[1] Faculty of Engineering, Kingston University, Roehampton Vale, Friars Avenue, London SW15 3DW, UK
[2] School of Computing & Mathematical Sciences, University of Greenwich, 30 Park Row, London SE10 9LS, UK

Received: 27 March 2006 / Received in final form: 3 October 2006 / Accepted: 8 November 2006
Published online: 17 January 2007 –

Abstract. This paper presents a numerical study of the Reynolds number and scaling effects in microchannel flows. The configuration includes a rectangular, high-aspect ratio microchannel with heat sinks, similar to an experimental setup. Water at ambient temperature is used as a coolant fluid and the source of heating is introduced via electronic cartridges in the solids. Two channel heights, measuring 0.3 mm and 1 mm are considered at first. The Reynolds number varies in a range of 500–2200, based on the hydraulic diameter. Simulations are focused on the Reynolds number and channel height effects on the Nusselt number. It is found that the Reynolds number has noticeable influences on the local Nusselt number distributions, which are in agreement with other studies. The numerical predictions of the dimensionless temperature of the fluid agree fairly well with experimental measurements; however the dimensionless temperature of the solid does exhibit a significant discrepancy near the channel exit, similar to those reported by other researchers. The present study demonstrates that there is a significant scaling effect at small channel height, typically $\leq$0.3 mm, in agreement with experimental observations. This scaling effect has been confirmed by three additional simulations being carried out at channel heights of 0.24 mm, 0.14 mm and 0.1 mm, respectively. A correlation between the channel height and the normalized Nusselt number is thus proposed, which agrees well with results presented.

PACS. 47.61.-k Micro- and nano- scale flow phenomena – 47.61.Fg Flows in micro-electromechanical systems (MEMS) and nano-electromechanical systems (NEMS)

1 Introduction

Advance in micromachining technology in recent years has enabled the design and development of miniaturized systems [1], which opens a promising field of applications, particularly in the medical science and electronic-/bio-engineering [2,3]. Such systems often contain small scale fluid channels embedded in the surrounding solids with heating sources. Depending on the channel height, it can be described as a minichannel (at a characteristic dimension of about 1 mm) or a microchannel (at a characteristic dimension of several microns to several hundred microns). Because of its undeniable advantages of smaller physical dimensions and higher heat transfer efficiency, the study of microchannel flows has become an attractive research topic with a fast-growing number of publications, for example the experimental study by Gao et al. [4] on the fundamental fluid dynamics in relation to the in-depth small scale physical phenomena.

Tuckerman and Pease [5] performed the first experimental study of the heat transfer in the microchannels with heat sinks some twenty years ago. Since then, numerous studies have been carried out both experimentally and numerically, to address the fundamentally important but practically difficult issues. One such theme was the enhancement of the heat transfer coefficient by varying the Reynolds number and decreasing the channel height to micron scale. Cobhan and Garimella [6] published a comprehensive review summarizing the research work carried out in this field.

To date, the experimental data reported in the open literatures show a significant scattering of results [6] which on occasions disagree with the conventional theories for transport phenomena, that have been well verified for macroscale flows. Previous experiments of microchannel often exhibited some controversial findings and sometimes even opposite trends, when compared to conventional channels, most notably the Reynolds number (Re) and the scaled channel height effects on the Nusselt number (Nu). As an example, Peng et al. [7] observed these two effects from a study of the heat transfer in a rectangular microchannel with hydraulic diameter ranging from 0.133 mm to 0.343 mm and Celata et al. [8] observed similar trends when studying a laminar flow in a capillary tube of 0.130 mm in diameter.

While the conventional theory indicates that for fully-developed laminar channel flow the Nusselt number should

[a] e-mail: y.yao@kingston.ac.uk

remain constant and is independent of the Reynolds number, this is not always correct for microchannel flows. In fact, a number of controversial findings have been reported by some researchers, who observed the *Re*-dependence of *Nu* variations, but others did not have the same conclusions. Here, a few typical cases are listed for comparisons.

- In a trapezoidal silicon microchannel experiment study, Qu et al. [9] confirmed that the conventional theory was still applicable even at a small microchannel height ranging from 62 microns to 169 microns of hydraulic diameter, where they have observed the *Re*-independent Nusselt number variations at very low value ($Nu \approx 1$–2).
- On the contrary, Wang and Peng [10] found that in laminar flow region the Nusselt number increased along with the Reynolds number, but were only 35% of those predicted by theory.
- The most trivial conclusion comes from Wu and Little [11], who revealed that the Nusselt number was lower for $Re < 600$, but became higher for $600 < Re < 1000$, when compared to the predictions by the conventional correlations.

The reasons leading to such diverse experimental observations are still not clear. It is quite likely that this phenomenon might be partly related to the entrance effects. Gao et al. [4] has recently carried out a carefully designed experimental study with a convergence channel inlet, in which entrance effects have been revealed.

The channel height effect in microchannels is also an arguable theme with contradictory conclusions. In the laminar regime, Qu et al. [9] observed the significant scaling effects on hydraulics in a trapezoidal channel at height of around 111 microns. On the contrary, Flockhart and Dhariwal [12] did not find the scaling effects for the same type of channel even at a lower channel height of around 63 microns. For rectangular shape microchannels, Gao et al. [4] reported an experimental study of the scaling effects on the hydrodynamics in both mini- and microchannel with similar findings as Qu et al. [9]. Guo and Li [13] also noted the significant scaling effects and suggested that the effects from the heat conduction, in the solid walls and the entrance of the microchannel, might be two possible sources of errors that might contribute to the deviation from conventional laws. Surprisingly, a recent comprehensive numerical study by Gamrat et al. [14] revealed that the scaling effects have not been observed even at a small channel height of 0.1 mm. Although the reason for this has not been clearly understood, it must be emphasized that adequate experimental measurements in microchannels are extremely difficult due to the small scale of the test sections. This is especially true for the heat transfer data acquisition as there is no direct measurement of the heat fluxes at the fluid-solid interface reported in published studies.

As discussed in [4], there are a few other factors which may also influence these controversial findings, particularly the electronic double layers (EDL) and the wall roughness effects. However, the EDL theory only gives about 5–10% reduction in the Nusselt number [4], which is exceptionally lower compared to a factor of 3 observed by Wang and Peng [10]. Furthermore the EDL effect can often be negligible when the channel height is greater than 40 microns [15]. The wall roughness effect was considered by Sabry [16] as a most possible factor to explain the observed results. A recent study by Qu et al. [9] has confirmed that good agreement between predictions and measurements can be achieved while taking this factor into account. Other effects like gas rarefaction [13] would only appear when the continuity assumption breaks down, but this might never be happened, because for majority of microchannels the hydraulic diameter will be larger than 0.1 mm. Based on these facts, the most common technique used to study microchannel flows is generally via the use of the conventional Navier-Stokes solutions, although this methodology may be arguable when the low limit of microscale of about 0.1 mm hydraulic diameter approaches. All simulations in this study have the scale larger than this limit; hence the Navier-Stokes solution is still applicable.

Following the experimental investigation of Gao et al. [4] and the numerical study of Gamrat et al. [14], the present study is devoted to a numerical study of microchannel flow combined with a conjugate heat transfer, which couples the fluid convection in a rectangular microchannel and the heat conduction in the solids. The numerical setup is chosen as close as possible to the configuration reported by Gao et al. [4]. The wall heat flux is assumed to be uniformly distributed over the fluid-solid interfaces. Two main objectives of the present study are (1) to compare the present predictions against the experimental data [4] and other numerical results [14], and (2) to verify the Reynolds number and the channel height effects on the deviation of the heat transfer from the classical corrections, which usually valid for macroscale flows.

2 Computational approach

2.1 Problem description

The physical problem considered here comes from a recent experimental investigation of the heat transfer in mini- and microchannels by Gao et al. [4]. Figure 1 illustrates the configuration used in the experimental setup. The active channel walls are two plane bronze blocks, separated by a stainless plate (at a thickness of 'e' which is the channel height) and a hollow section (at a width of 'w' and a length of 'L' in size) at the centre. Two rectangular chambers are machined in the solid blocks with inlets and outlets. The chambers are also linked to the entrance and the exit of the channel.

The main advantage of this setup is that the channel height can be easily adjusted by varying the steel plate thickness in a range of 0.1–1 mm in steps of 0.1 mm each time. The heat sinks are introduced with the aid of four square shaped electric cartridges, which are embedded symmetrically inside the two solid blocks and surrounded with insulating materials. The length of electric cartridges is slightly shorter than the microchannel length L. It is

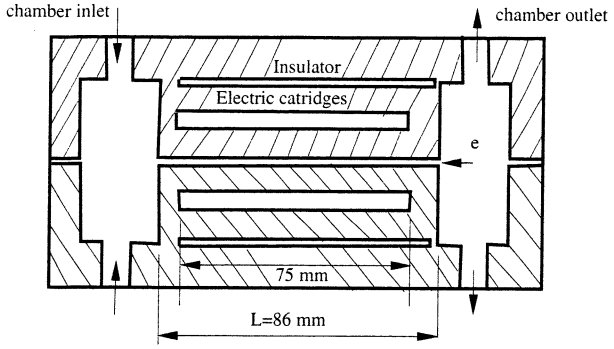

Fig. 1. Sketch of configuration with views at the middle cross-section plane.

worth noting that there are a few differences in the current setup comparing to that by Gao et al. [4]. The geometry of the entrance in the upstream direction, i.e. the joint plane between the chamber and the microchannel entrance has a rectangular shape and has not been rounded off as did in [4]. The main reason for this is to achieve a uniform inlet velocity profile and minimise any possible distortions at the channel entrance, two square inlets are used also to ensure the flow remains symmetric. Heat losses from such a design are mainly concentrated at the channel exit as the heat sinks are about 25% shorter than the channel length. The mass flow rate at two inlets is set to be equal and the sum matches the experiment data of Gao et al. [4]. The solid blocks are assumed to be made of similar material as that in the experiment. Details of the experimental setup can be found in reference [4].

2.2 Computational domain and meshing procedure

Based on the configuration described in above, a computational domain was prescribed, which combined two components; the fluid flow part consisting of two chambers each having own inlet and outlet and linked with a flow channel, and the solid part surrounding the flow channel and chambers embedded with four square shaped heat sinks. Because of the topology of this geometry, a multi-block structured mesh was generated and at each rectangular shaped sub-domain, a good quality structured mesh was prescribed to achieve "good" numerical accuracy and efficiency for the solution. Across the sub-domains (i.e. the fluid and solid domains), mesh lines were joined together without introducing any numerical errors due to the interpolation. A number of grids were used to obtain grid-independent results. Details of domain setup and meshing process can be found in [17].

2.3 Numerical method and boundary conditions

Numerical simulations of this typical combined conjugate heat transfer and fluid flow problem were carried out using the commercial CFD package PHOENICS version 3.4 [18]. The governing equations for fluid flow were solved by means of the commonly adopted finite volume methodology and the pressure-velocity coupling technique of SIMPLE algorithm for satisfying the continuity of flow field. The algorithm allows that the convective fluxes per unit mass through cell faces could be evaluated from the guessed velocity, whilst the momentum equations and a pressure correction equation were solved via a pressure field. The process has been iterated and progressed until the converged velocity and pressure fields have been achieved. Due to the low Reynolds number, the fluid (water) in the domain was assumed to be incompressible, which exhibited laminar flow characteristics with constant flow properties. Furthermore the buoyancy forces and radiation effects were neglected. Heat transfer in the solid blocks was solved by the heat conduction equation, providing the constraints in terms of boundary conditions for the flow solution.

By using water at ambient temperature as the coolant, the Navier-Stokes equations were solved under the hydraulic boundary condition of uniform flow velocity at the two inlets. The thermal boundary conditions used for solving the energy equation and the heat conduction were:

- The heat flux supplied by four electric cartridges was defined as 180 W, and was kept constant during the solution process. The heat source appears to be uniformly distributed over the electric cartridges and the heat flux distributions over the solid-fluid interface is determined by the solution of temperature field in the solid.
- There existed free convective heat transfer with the surrounding air on the outside walls of domain. An ambient temperature of 300 K was defined as a reference value and a heat transfer coefficient of 10 $\mathrm{W\,m^{-2}\,K^{-1}}$ was chosen.
- Adiabatic wall conditions were prescribed for the remaining surfaces.

2.4 Solution procedure

Simulations on a series of grids at various densities were carried out in order to identify a baseline mesh, which would provide grid-independent solutions. For each computation, the convergence criteria for the streamwise, spanwise and wall-normal velocity components were set to achieve the residual of 10^{-5}, and in most cases, the residual of spanwise velocity component could achieve 10^{-6} after 500 iterations. The final baseline mesh utilized 98 400 cells for all simulations (with varying channel height of 0.3–1 mm), that was $164 \times 30 \times 20$, in streamwise, spanwise and wall-normal respectively. This grid resolution was comparable to that used by Gamrat et al. [14] in their numerical study, in which they found that the computed channel velocity profile has very little difference between the grids of 20, 30 and 40 along the channel height. However, there did appear to be some differences between 80 and 164 nodes in the channel streamwise direction. Thus, the higher limit of 164 nodes was used in the present study. As the problem was "basically" two-dimensional, there were no significant influences from a

spanwise resolution. For validation purpose, a trial simulation of the laminar flow at a Reynolds number of 2166 was performed and the results were compared with that by Gamrat et al. [14]. In general, the predicted temperature distributions agree reasonably well with those reported by Gamrat et al., e.g. a predicted value of 295.8 K at the channel entrance, exactly the same as that given in [14], and a predicted value of 296.7 K at the channel exit, about 0.4 K lower than that obtained by Gamrat et al.

3 Results and discussions

Previous study by Gamrat et al. [14] found that the characteristics of the fluid flow and the heat transfer in the microchannel had significant dependency on the Reynolds number and the Prandtl number. In this study, we concentrate on two key issues. These are (1) the variations of the Nusselt number along the channels axial direction and (2) the effect of microchannel height when it reduces down to 0.3 mm. As a uniform inlet profile is prescribed, the entrance effect as studied by Gamrat et al. [14] will not be investigated here. The Reynolds number applying the averaged velocity (V_{ave}) as the characteristics velocity and the hydraulic diameter (D_h) as the characteristics length, which can be evaluated via the formula

$$D_h = \frac{4 \times C_A}{W_p} \tag{1}$$

where C_A is the cross-sectional area and W_p represents the wetted perimeter, both at the channel entrance. The Reynolds number considered varied in a range of 500 to 2200, similar to that used in the experimental investigation of Gao et al. [4] and the numerical study of Gamrat et al. [14].

3.1 Model validation against theory

The numerical model as described in above was validated against a theoretical estimation for simultaneously thermally and hydraulically fully-developed laminar flow along a two-dimensional channel with symmetrical uniform heat flux surfaces. The theoretical solution reported by Shah and London [19] was suggested by Bejan and Sciubba [20] using empirical formulas proposed by Churchill and Usagi [21]. Numerical simulations were carried out at Prandtl number of 0.7, for which the local Nusselt number was defined as (assuming a uniform inlet velocity and temperature),

$$Nu = \frac{\phi \times D_h}{(T_w - T_f)k} = [(0.587(x^*)^{-0.5})^3 + 8.235^3]^{1/3} \tag{2}$$

where ϕ is the heat flux. T is the temperature with subscripts 'w' stands for wall and 'f' for fluid. k is the local thermal conductivity. The dimensionless abscissa is defined as $x^* = x/(D_h RePr)$.

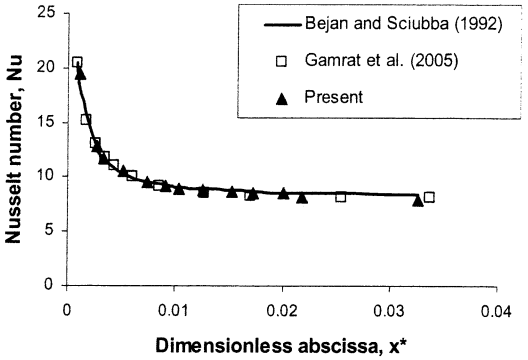

Fig. 2. Comparison of local Nusselt number (Nu) between the theoretical estimations, the predictions by Gamrat et al. [14], and the present results.

The predicted local Nusselt number from the simulations can be evaluated via the heat transfer coefficient given by [4] as

$$h = \phi/(T_w - T_f) \tag{3}$$

$$\phi = P/(2wl_h) \tag{4}$$

$$T_f = T_{in} + (T_{out} - T_{in})x/l_h \tag{5}$$

$$Nu = \frac{hD_h}{k} \tag{6}$$

where h is heat transfer coefficient. P is electric power in Watts. The 'w' is the width of the channel. The l_h is the heating resistant length. The subscript '*in*' represents the inlet and '*out*' stands for the outlet.

Figure 2 presents the comparisons of local Nusselt number variations along the channel axial direction for $Re = 832$, $Pr = 0.7$ and $e = 1$ mm. It can be seen that the present numerical predictions show excellent agreement with theory of Bejan and Sciubba [20] and the predictions by Gamrat et al. [14] with uniform inlet profile for the same problem.

3.2 Reynolds number effects on Nusselt number

Figure 3 presents the Nusselt number variations as a function of dimensionless coordinate x^* along the channel axial direction for two sets of conditions: (1) the Reynolds numbers ranging from 518 to 2076 and the channel height of 1 mm; and (2) the Reynolds numbers ranging from 506 to 2023 and the channel height of 0.3 mm, respectively. The Prandtl number is fixed for 6 for all cases. The theoretical curve based on $Pr = 6$ from Shah and London [19] and the numerical predictions by Gamrat et al. [14] at the same Reynolds numbers are also plotted in the figure for comparisons.

Figure 3a shows the comparisons of numerical predictions and theoretical estimation for the channel height of 1 mm. At high Reynolds number of 2076, present numerical results agree reasonably well with the theory, despite minor deviations exist near the exit where the influences from the heat sinks are evident. At two low Reynolds numbers of 518 and 865, the predictions exhibit some noticeable deviations at both the entrance and the exit of the

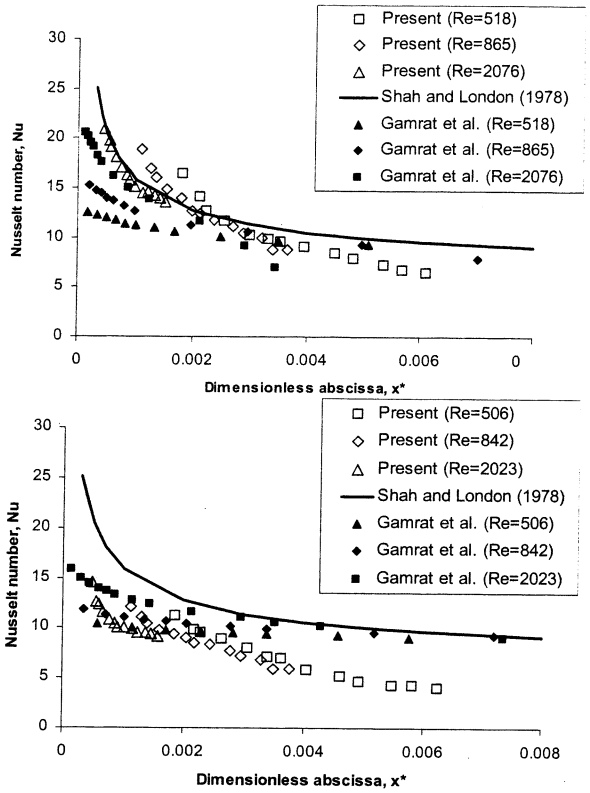

Fig. 3. Variations of the Nusselt number at various Reynolds numbers and channel heights of (a) $e = 1$ mm (upper) and (b) $e = 0.3$ mm (lower).

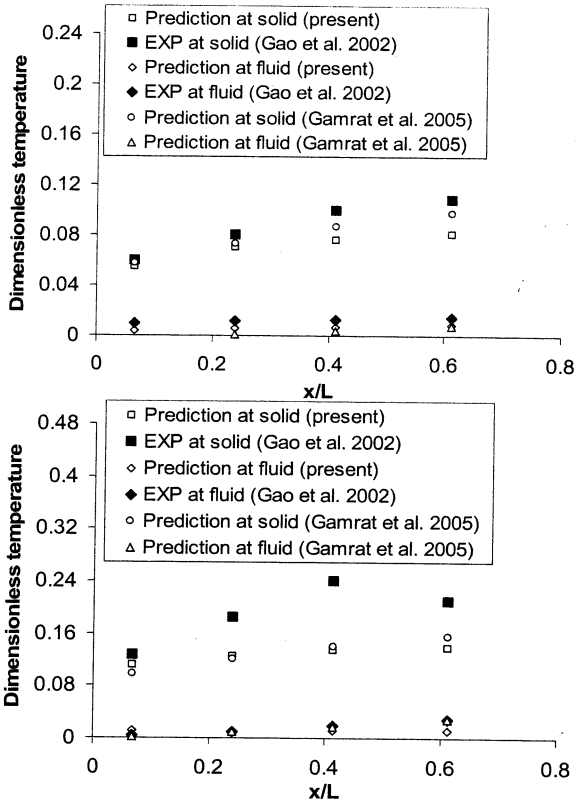

Fig. 4. Comparison of the dimensionless temperature between the experimental data and the numerical predictions for the wall and the bulk of fluid along the channel axial direction. (a): $e = 1$ mm and $Re = 2166$ (upper) and (b): $e = 0.3$ mm and $Re = 2061$ (lower).

channel, which could be attributed to the local sudden contraction and expansion effects. The results of Gamrat et al. [14] also show some good agreements with the theory at high Reynolds, but relative poor comparisons at low Reynolds numbers with some deviations at the channel entrance. Downstream near the exit the results agree the theory slightly better than our predictions, probably due to a convergence shape used in their study.

Figure 3b gives the results for the channel height of 0.3 mm. It is clear that for three Reynolds numbers considered, our predictions have some downwards 'drift' when compared to theoretical predictions; however the overall profiles and trends are quite similar. This 'drift' effect has been discussed by Gao et al. [4] in their experimental study and it was concluded that this can be attributed to the changes in channel heights, i.e. scaling effects, which will be discussed in more details later. The results of Gamrat et al. [14] present similar downwards 'drift' near the channel entrance, but downstream such a 'drift' gradually disappears and the results agree the theory fairly well and no scaling effect has been claimed from their study.

For both channel heights, apart from the channel entrance portion, the numerical results by Gamrat et al. [14] agree with the theory quite well with no scaled height effect at small channel height of 0.3 mm. They even claimed that no significant scaling effect was observed at a smaller channel height of 0.1 mm. In contrary to their numerical predictions, the present studies indicates that scaling effects on the heat transfer performance at the channel entrance and along the channel do appear at small channel height of 0.3 mm and they are dependent on the Reynolds number. This observation is in agreement with the experiments of Gao et al. [4]. The possible causes of this scaling effect will be discussed in later sections.

3.3 Comparison with experimental measurements

The comparison of dimensionless temperature distribution between the numerical predictions of this study and the experiment data of Gao et al. [4] is illustrated in Figure 4 for the channel heights of 1 mm and 0.3 mm, respectively. The dimensionless temperature (θ) is calculated as follows:

$$\theta = \frac{(T - T_{in}) \times k}{\phi \times D_h} \tag{7}$$

where T can be either T_f (the subscripts 'f' represents 'fluid') or T_s ('s' means the solids).

Figure 4 presents the distributions of θ along the channel axial direction for both the fluid and the solid domains. It can be seen that the discrepancies between experimental results and numerical predictions for the bulk water temperature T_f (diamond symbols in Figure 4a, unfilled

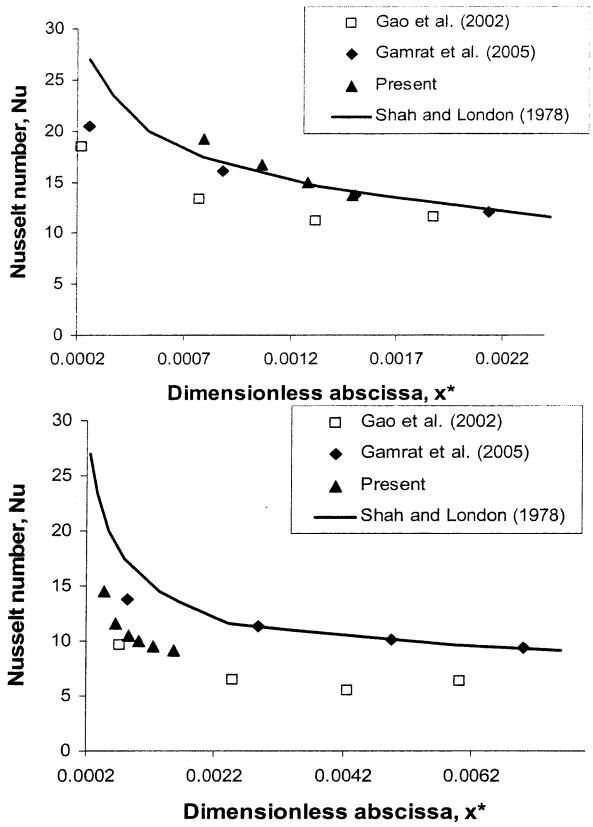

Fig. 5. Comparisons of the Nusselt number along the channel between the experimental data [4], the numerical predictions from Gamrat et al. [14] and the present results. (a): $e = 1$ mm and $Re = 2166$ (upper) and (b): $e = 0.3$ mm and $Re = 2061$ (lower).

for predictions and filled for test data) are quite small. This helps to verify the use of the assumption of linear variation of T_f. However, larger discrepancies do occur in the solid region (square symbols in Fig. 4b, unfilled for predictions and filled for test data) resulting in higher values of the difference between the fluid and the walls for the experimental results. For $e = 1$ mm, the discrepancies between experimental and numerical results vary between 8% and 25%, when compared to the experimental data, while for $e = 0.3$ mm they increase to a maximum value of 44%. Gamrat et al. [14] reported similar findings in their recent numerical studies. The reason for causing such a significant discrepancy is not clear; nevertheless some of the error can be attributed to both difficulties and inaccuracies in the measurements [14].

Figure 5 presents the Nusselt number variations against the dimensionless of the channel length for two settings, (a) $e = 1$ mm and $Re = 2166$ and (b) $e = 0.3$ mm and $Re = 2061$. Although the predictions have a similar trend, the present results are still lower than theoretical values for the channel height of 0.3 mm. For $e = 1$ mm, the numerical predictions from present study and that of Gamrat et al. [14] agree reasonably well, and both over-predict the experimental data by some 30%. For $e = 0.3$ mm, the present predictions are closer to the test

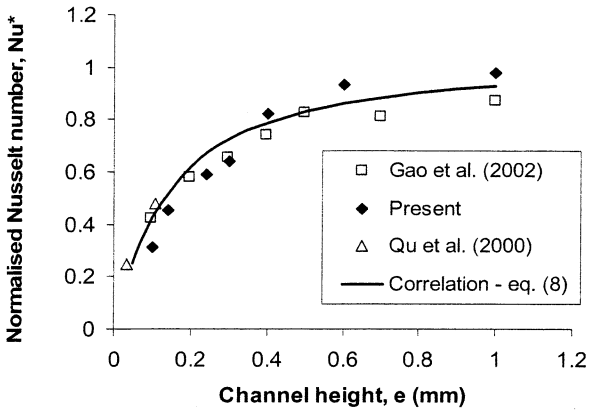

Fig. 6. Effect of channel height on the Nusselt number with comparison to the experimental data of Gao et al. [4], Qu et al. [9] and present numerical predictions.

data, while that by Gamrat et al. [14] tend to approach theoretical values. This discrepancy may be attributed to several factors. As discussed by Gamrat et al. [14], two of these could be the entrance difference and the wall roughness, which can lead to differences in the fluid properties and the convective heat transfer characteristics in the microchannel. Qu et al. [9] performed a study accounting for the wall roughness effect, which leads to a better comparison with the experiment data been achieved.

3.4 Correlation of scaling effects

The experimental study of Gao et al. [4] reported that there was a significant channel height effect on the local Nusselt number variations. Although previous numerical study by Gamrat et al. [14] did not verify this observation, even for very lower channel height of 0.1 mm, it is worth checking this from the present study. For this purpose, we have conducted further three simulations with smaller channel heights of 0.24 mm, 0.14 mm and 0.1 mm. Similar to that reported in [4], the value of Nu_{av} was derived by averaging the Nu at the three experimental thermocouple locations, to study the influence of the channel height.

Figure 6 presents the normalised Nussult number ($Nu^* = Nu_{av}/Nu_{th}$) for $x^* = 0.02$ as a function of the channel height, where Nu_{th} is the theoretical value of Nusselt number [22] for the same value of x^*. It can be seen that a fairly good agreement has been achieved in the present simulations with slightly over-predictions at larger channel heights of 0.6 mm and 1 mm. It is worth noting that at the channel height of less than 0.3 mm, the present study simulation does show the significant scaling effect on the Nusselt number, in agreement with the experimental observations by Gao et al. [4]. At the present time, the physical mechanisms for the scaling effect on Nusselt number variation is still under-investigation. Guo and Li [23] suggested one possible reason is that as the characteristic length decreases, the variations of the predominant factors could influence the relative importance of flow and heat transfer phenomena.

Based on our simulation results and the experimental data of Gao et al. [4] and Qu et al. [9], a correlation is proposed which takes the form as presented in equation (8). The correlation is a very good fit to the data from various other studies.

$$Nu^* = \frac{0.93e^2}{0.00119 + 0.11643e + 0.88238e^2}. \quad (8)$$

4 Conclusions

A rectangular microchannel flow has been studied numerically by using a three-dimensional CFD model. The geometry chosen is similar to that used in the experimental study of Gao et al. [4] and the numerical study of Gamrat et al. [14]. Numerical computations have been carried out for a combined conjugate heat transfer and fluid flow problem, by considering the coupling between the convective heat in the microchannel fluid and conductive heat on the walls and in the surrounding solid blocks. A detailed study of the heat transfer characteristics, in terms of the Nusselt number dependency on the Reynolds number and the channel height are presented in this paper. The following conclusions can be drawn from this present study:

- The predicted temperature shows that temperature at the channel entrance has a value of 295.8 K, same as that reported by Gamrat et al. [14]. At the channel exit, the predicted temperature is 296.7 K, which is about 0.4 K lower compared to the results of Gamrat et al. [14].
- The variations of Nusselt number, as a function of dimensionless length, are overall in good agreement with the analytical results based on the conventional continuum theory (Bejan and Sciubba [20]), in which the uniform inlet profile is assumed. However for a fully-developed inlet profile, Gamrat et al. [14] observed that the channel entrance influence can not be neglected.
- The numerical prediction indicates that the Nusselt number decreases with the Reynolds number for channel heights of 0.3 mm and 1 mm. The discrepancy between theory and prediction increases while the channel height decreases.
- Although the dimensionless fluid temperature agrees fairly well with the experimental data, the predicted value in the solid blocks has significant discrepancy compared to the results reported by Gao et al. [4]. The reason for this is still not clear yet, although the present findings are agreed with the numerical study of Gamrat et al. [14].
- In contrary to the results of Gamrat et al. [14], the present study reveals significant scaling effects on the Nusselt number for a channel height of 0.3 mm. Nevertheless, this finding is in good agreement with the results of Gao et al. [4] and Qu et al. [9].
- A new correlation is proposed for the Nusselt number dependency on the channel heights, which compares well with experimental data.

In conclusion, the numerical study implies that the heat transfer performance in microchannels can be largely enhanced by scaling down the channel height to micron size. Conventional theory can be used only for the channel height of no less than 0.3 mm, while below this limit the scaling effects will appear. The accuracy of numerical predictions for micrometer sized channel is crucially dependent on the boundary conditions and other properties such as the wall roughness. Thus one should be cautious when comparing the results with the experimental data. The future work will focus on other characteristics such as Poiseuille number, laminar friction coefficient.

References

1. C.-M. Ho, Y.-C. Tai, Annu. Rev. Fluid Mech. **30**, 579 (1998)
2. T. Chovan, A. Guttman, Trends Biotechnol. **20**, 116 (2002)
3. B. Gromoll, Rev. Gen. Therm. **37**, 781 (1998)
4. P. Gao, S. Le Person, M. Favre-Marinet, Int. J. Therm. Sci. **41**, 1017 (2002)
5. D.B. Tuckerman, R.F.W. Pease, IEEE Electr. Device L. **5**, 126 (1981)
6. C.B. Sobhan, S.V. Garimella, Microscale Therm. Eng. **5**, 293 (2001)
7. X.F. Peng, G.P. Peterson, B.X. Wang, Exp. Heat Transfer **7**, 265 (1994)
8. G.P. Celata, M. Cumo, M. Guglielmi, G. Zummo, Microscale Therm. Eng. **6**, 85 (2002)
9. W. Qu, M. Mala, D. Liu, Int. J. Heat Mass Tran. **43**, 3925 (2000)
10. B.X. Wang, X.F. Peng, Int. J. Heat Mass Tran. **37**, 73 (1994)
11. P.Y. Wu, W.A. Little, Cryogenics **24**, 415 (1984)
12. S.M. Flockhart, R.S. Dhariwal, J. Fluids Eng.-T. ASME **120**, 291 (1998)
13. Z.Y. Guo, Z.X. Li, Int J. Heat Mass Tran. **46**, 149 (2003)
14. G. Gamrat, M. Fravre-Marinet, D. Asendrych, Int. J. Heat Mass Tran. **48**, 2943 (2005)
15. L. Ren, W. Qu, D. Li, Int. J. Heat Mass Tran. **44**, 3125 (2001)
16. M.N. Sabry, in *Proceedings of Conf. Therminice, Rome, Oct. 1999*
17. J. Yao, Y.F. Yao, M.K. Patel, P.J. Mason, in *Proceddings of 13th Int. Heat Transfer Conf., August 2006, Sydney, Australia*
18. PHOENICS version 3.4 user's manual, CHAM Ltd. 2001
19. R.K. Shah, A.L. London, *Advanced Heat Transfer* (Academic Press, New York, 1978)
20. A. Bejan, E. Sciubba, Int. J. Heat Mass Transfer **35**, 3259 (1992)
21. S.W. Churchill, R. Usagi, AICHE J. **18**, 1121 (1972)
22. F.M. White, *Viscous Fluid Flow*, 2nd edn. (McGraw-Hill, New York, 1991)
23. Z.Y. Guo, Z.X. Li, Int. J. Heat Fluid Fl. **24**, 284 (2003)